esa

ECOSPHERE

The ecology of infection between a transmissive and a dead-end host provides clues for the treatment of a plant disease

MATTEO GARBELOTTO,[1] DOUG SCHMIDT,[1] STEVEN SWAIN,[1,2] KATHERINE HAYDEN,[1,3] AND GUGLIELMO LIONE[1,4,†]

[1]*Department of Environmental Science, Policy, and Management (ESPM), University of California at Berkeley, 54 Mulford Hall, Berkeley, California 94720 USA*
[2]*University of California Cooperative Extension (UCCE), 1682 Novato Blvd., Suite 150B, Novato, California 94947 USA*
[3]*Royal Botanic Garden Edinburgh, 20A Inverleith Row, Edinburgh, EH5 2EG, Scotland, UK*
[4]*Department of Agricultural, Forest and Food Sciences (DISAFA), University of Torino, Largo Paolo Braccini 2, I-10095, Grugliasco, TO, Italy*

Citation: Garbelotto, M., D. Schmidt, S. Swain, K. Hayden, and G. Lione. 2017. The ecology of infection between a transmissive and a dead-end host provides clues for the treatment of a plant disease. Ecosphere 8(5):e01815. 10.1002/ecs2.1815

Abstract. In plant pathosystems in which some hosts are transmissive and some are dead-ends, infection is mediated by multiple factors including the susceptibility of both hosts, the sporulation potential of transmissive hosts, the mobility of infectious propagules, the presence of environmental factors conducive to infection, and the variability in distribution of both host types. The factors above were studied for the California forest disease sudden oak death caused by the pathogen *Phytophthora ramorum*. This pathogen is exotic to California, and while it sporulates at significant levels on the leaves of California bay laurels, four susceptible oak species appear to be non-infectious dead-end hosts. Here, we report, for the first time, on inoculum levels necessary to successfully infect adult oaks and on the distribution of such inoculum levels through time and space thanks to a seven-year-long monitoring effort across a network of 128 monitoring points. Through a series of geostatistical and statistical analyses, we show that the presence of high inoculum loads is positively correlated with close proximity to bay laurels, with high rainfall levels, and with warmer temperatures. Data are consistent with splash dispersal of the pathogen and show that increased presence of tanoak corresponds to a reduced presence of bay laurels and to a lower frequency of high inoculum events. Removal of bay laurels resulted in a substantial decrease of number of events in which spore loads were high enough to infect oaks. This effect was significant when bays were removed 10 m around sampling points, thus indicating that removal of bays 10 m around oaks is a valid approach to reduce infections of oaks.

Key words: epidemiology; forest disease; infectious host; inoculum dilution; inoculum threshold; non-infectious host; *Phytophthora ramorum;* sporulation; sudden oak death; susceptibility.

Received 9 December 2016; revised 23 March 2017; accepted 24 March 2017. Corresponding Editor: Debra P. C. Peters.

† **E-mail:** guglielmo.lione@unito.it

INTRODUCTION

Infectious diseases can affect single or many hosts (Poisot et al. 2011). When multiple hosts can be infected, two alternate scenarios may describe disease dynamics: In the first one, all hosts are infectious and hence transmissive, while, in the second, some of the hosts are not infectious and thus are normally defined dead-end hosts (Reisen 2010). Zoonotic and vector-borne diseases generally include several examples that fall into this second category, and a rich body of literature is available on the various aspects of their epidemiological cycle (Kilpatrick and Randolph 2012). In particular, a lot of emphasis has been placed on understanding how transmission is regulated between transmissive and dead-end hosts, including the role played by varying biodiversity

levels, by hosts that amplify infectious inoculum, and by those that act as reservoirs of inoculum (Weaver and Barrett 2004, Keesing et al. 2010, Tersago et al. 2010, Funk et al. 2013). With the exception of insect-vectored plant diseases, there are relatively few clear cases of infectious plant diseases that fall into the second scenario, and the literature on their ecology is relatively wanting (Alma et al. 2000, Morilla et al. 2005). Evidence gathered from studies on the plant disease sudden oak death (SOD) suggests that this disease actually falls into both scenarios, depending on the habitat that is affected (see Garbelotto and Hayden 2012).

Sudden oak death in California is an invasive infectious disease caused by the exotic pathogen *Phytophthora ramorum* Werres, De Cock & Man in't Veld (Rizzo et al. 2002). In the 1980s and 1990s, before it was identified, the pathogen was transported from its unknown native range to North America and Europe, as well as between North America and Europe through infected ornamental plants (Grünwald et al. 2012). A genetic epidemiological approach has demonstrated that *P. ramorum* has escaped from ornamental plants into natural California habitats at least 12 times (Croucher et al. 2013). Because of these multiple introductions, the current range of SOD in California is rather extensive (Garbelotto et al. 2014).

Over one hundred plant species have been identified as hosts for *P. ramorum*, including a large number of native California species (Garbelotto et al. 2003). By analyzing presence or absence of sporulation in natural infestations, it has been possible to discover that oaks (*Quercus* spp.) support minimal or no sporulation, while spores are abundant on the leaves of California bay laurels [or bays, *Umbellularia californica* (Hook. & Arn.) Nutt.], and to a lesser degree, they are produced on the leaves and twigs of tanoaks [*Notholithocarpus densiflorus* (Hook. & Arn.) Manos, Cannon & S.H. Oh] and on the needles of redwoods [*Sequoia sempervirens* (D. Don) Endl.] (Davidson et al. 2005). Thus, in the mixed evergreen forests of California, oaks act as dead-end hosts, while California bay laurels are the major transmissive hosts representing the primary reservoir host for *P. ramorum* inoculum (Davidson et al. 2008). Bay laurels are common in western North America, growing as shrubs or trees both in open spaces and under the canopy of other species, in a wide range of habitats with different soil and climate conditions (Goralka and Langenheim 1995). Despite an obvious parallel between SOD and zoonotic diseases, transmissive hosts such as California bay laurels do not move like pathogen vectors do. Hence, transmission between hosts is regulated by the spore load necessary to infect a dead-end host, by the sporulation potential of the transmissive host, and by the effective mobility of the infectious propagules themselves. All of the above parameters of course, as in the case of zoonotic diseases, are modulated by environmental parameters (Grenfell and Dobson 1995). This study attempts to identify those parameters, both biological and ecological, that regulate transmissive-to-dead-end host infection. The most important infectious propagules for the spread of *P. ramorum* are called sporangia. These are ovoid asexually produced structures, approximately 50 $\times$ 25 μm, that become airborne supposedly through splash associated with rain events. Once they land on a wet plant surface, sporangia release 20–30 biflagellate motile zoospores that are responsible for host infection (Werres et al. 2001). When using the term "inoculum" in this study, we refer to sporangia and to the zoospores that emerge from them.

The studies described in this paper were designed to answer some of the key epidemiological aspects of oak infection by the SOD pathogen, and to test the efficacy of selective bay removal around oaks as a preventive disease management strategy. Oaks and bay laurels are sympatric in most of their ranges and it has been observed that SOD-infected oaks are strongly associated with bay laurels, but the cause of this spatial pattern is yet to be determined (Kelly and Meentemeyer 2002, Liu et al. 2007, Swiecki and Bernhardt 2008). Despite our ignorance of the reasons behind the proximity of infected oaks to bays, removal of bays in the 2- to 10-m range has been suggested as a possible way to interrupt the final step of the oak infection pathway (Swiecki and Bernhardt 2008). However, there is no experimental evidence the approach would be effective.

The close proximity of infected oaks to bays may depend on two concurrent factors: (1) A large number of propagules may be required to successfully infect oaks and (2) dispersal of infectious propagules may be spatially limited, resulting in clouds of high inoculum levels only near a source, for example, an infected bay. Population genetic studies have shown that genetic similarity decreases

sharply with distance from a source, suggesting that propagules do not travel large distances (Mascheretti et al. 2008). However, when spatial autocorrelation analyses were repeated in different years or seasons, thresholds of allelic overaggregation were 10 m in dry years, but increased to at least 200 m in wet years (Eyre et al. 2014). It should be noted that these studies are based on isolations of the pathogen from bay laurel leaves, and it has been shown that even low numbers of propagules can cause foliar infections (Hüberli et al. 2008). Thus, the values reported in the literature may apply to the movement of low numbers of propagules, but may be uninformative on patterns of high inoculum levels. It is also possible that tanoak leaves may represent an additional source of infection for oaks, even if an association between infected oaks and tanoaks has yet to be reported.

Many studies have investigated the role played by ecological and climatic factors on SOD spread. Results have shown that disease spread is positively correlated with bay and tanoak density, and with rainfall, while correlation with temperature appears to be negative (Davis et al. 1998, Meentemeyer et al. 2008, Cobb et al. 2010). Most of these analyses, however, were based only on bay and tanoak infection and not on the dynamics of bay-to-oak infection. Generally, sporulation has been measured either by monitoring new infections (Eyre et al. 2013, Meentemeyer et al. 2015) or by using rainwater traps (Davidson et al. 2005). Studies using this second approach have proven inoculum is rain-borne; nonetheless, measurements using rainwater catches obviously cannot show that inoculum is absent when rainfall is missing. This question is particularly relevant because in many coastal woodlands of California, fog drip is significant during the dry months (Dawson 1998) and would easily provide the film of water that is necessary for effective infection by *P. ramorum*.

Under the above premises, and considering the gaps of knowledge on disease transmission between transmissive and dead-end host plants, we use the bay–oak SOD pathosystem as a model system to investigate the specific aims below:

1. to determine the threshold level of inoculum necessary for successful oak infection;
2. to design and test a new and robust approach to quantify the inoculum pressure of *P. ramorum* independent of rainfall;
3. to assess the frequency of events in which the above threshold is reached in a natural setting and to test for the presence of associations between these events and climatic variables;
4. to investigate the spatial pattern of the oak-infectious inoculum and to assess its relation to forest stand characteristics such as species composition and density; and
5. to determine whether removing bays in a 10- or 20-m buffer around oaks will sufficiently reduce inoculum pressure to prevent oak infection.

Methods

Determination of inoculum pressure necessary to infect oaks

A total of 12 large coast live oaks in boxes were purchased—four in March 2010 and eight in September 2011—and transported to a warehouse at the UC Berkeley Richmond Field Station (Richmond, California, USA). Their average diameter at breast height was 19 cm (range: 16–21). Trees were placed at the experiment site for 2 weeks prior to each experiment. Four trees were inoculated on 22 April 2010, while the remaining eight were inoculated on 28 October 2011. Temperature and relative humidity ranged between 12.8°C and 23.9°C and between 77% and 81%, respectively, during the course of both experiments. Each tree was inoculated with four different concentrations of zoospores of *Phytophthora ramorum* isolate Pr52 (Browning et al. 2008), namely 0, 10^3, 10^4, and 10^5 zoospores mL^{-1}. Each zoospore concentration was inoculated four times on the tree at 10, 30, 50, and 90 cm from the root collar. While each zoospore concentration was inoculated at all four heights on the stem, exact inoculation spots were randomized to avoid any bias. Zoospores were produced and counted as described in Eyre et al. (2014). Inoculations were performed as follows. The surface of the bark was lightly misted with deionized water 30 min before the inoculation. At each inoculation point, a 1 mm diameter × 0.5 mm deep hole was made in the bark; a zoospore inoculator (Appendix S1: Fig. S1) was attached to the bark using grafting wax, with the zoospore dispensing aperture on the side of the applicator perfectly matching the opening generated with the needle. The applicator reservoir was then filled with 1 mL

of zoospore suspensions, by pipetting zoospore suspensions through the reservoir access aperture on top of the applicator. The top opening of each zoospore dispenser was sealed with a rubber stopper to slow down evaporation and applicators were removed 48 h post-application. Six weeks after inoculation, the bark around each inoculation point was gently scraped, the size of the underlying necrotic stem lesion was measured vertically and horizontally, and the surface area of the stem lesion was calculated assuming an elliptic shape. Four isolations per inoculation point were performed by placing a small chip from the margins of the visible stem lesion onto Petri dishes filled with PARP (pimaricin + ampicillin + rifampicin + pentachloronitrobenzene [PCNB] agar) *Phytophthora* selective growth media. *Phytophthora ramorum* was identified morphologically and only stem lesions whose isolations were positively identified as *P. ramorum* were used in the ANOVA comparing stem lesion sizes (mm^2) obtained with inocula at different concentrations of zoospores. Multiple comparisons were made using Tukey's test, and data from each of the two trials were analyzed independently.

Development of a robust baiting approach for airborne propagules

Inoculum pressure was quantified through a spore trapping method designed ad hoc to collect *P. ramorum* propagules even in the absence of rainfall. Each trap consisted of a white polypropylene plastic bucket: The volume of each bucket was 14 L, and the diameter of the opening of each bucket was 29 cm. Buckets were filled with 1 L of deionized water every three weeks. During the experiment, buckets were covered with galvanized steel wire mesh with a mesh size of four openings/2.54 cm (1/4 in hardware cloth). The wire mesh prevented infected plant debris from dropping onto the water, thus avoiding an overestimation of actual airborne inoculum, and additionally prevented the bait leaves from exiting the buckets, in case of overflow. Buckets were replaced at each sampling time. Between samplings, the buckets were scrubbed with a plastic brush to remove organic matter, washed in a commercial greenhouse plant pot washing machine, and rinsed with deionized water before reuse. Immediately after pouring the water into the collection buckets, five healthy California bay laurel leaves were floated on the surface. All leaves were one year old, and all were from a single tree on the Berkeley campus, a location still uninfested during the entire course of the experiment. Floating of leaves was achieved by inserting the basal end of each leaf in a sandwich composed of a 1 cm thick × 6 cm diameter expanded polypropylene float, between two thin rubber washers, and tightened together with a short plastic nut and bolt. The final appearance of the bay leaves was that of a five-petal daisy, with each petal represented by a leaf. Any plant part susceptible to infection by *Phytophthora*, including fruits, can be used as baits, but bay laurel leaves were preferred because of their epidemiological importance in California and because they are hardy and do not decompose easily. Baiting is meant to attract motile zoospores of the pathogen that are released from sporangia and aggregate on the aerobic top layers of any body or film of water. Infection has been shown not to be random, but to be mediated by chemotaxis, a mechanism through which zoospores are attracted toward an available substrate (Oßvald et al. 2014).

Baiting periods were three weeks long. At the end of the bait period, when new fresh water and new bait leaves were added to the buckets, leaves were collected and brought to UC Berkeley where they were incubated for 2–4 d in a moist chamber with relative humidity (RH) >90%. Visible necroses were then plated on PARP-selective growth medium, and morphological observation of colonies growing on plates was used to differentiate between necroses caused by *P. ramorum* and those caused by other disease agents. Under the assumption that the number of infected leaves is proportional to the concentration of zoospores in the bucket, and that the secondary infections (if present) occur mostly within the same leaf, the number of infected leaves was used as a metric to assess the number of airborne sporangia produced.

The above assumptions and the relationship between number of infected bait leaves and inoculum pressure were tested by setting up three trials in an enclosed temperature-controlled room (18°C, 50% RH) at the UC Berkeley Richmond Field Station, Richmond, California, USA. Three buckets in the first trial (a total of 12 buckets) and eight in the other two trials (a total of 32 buckets per trial) were filled each with 1 L of deionized water and set in four rows of 10 buckets. Each bucket was then inoculated by adding

314 mL of water amended with four different concentrations of zoospores (0, 10^3, 10^4, and 10^5 zoospores mL^{-1}). The amount of water to be added was determined by calculating the surface area of the water in the bucket and multiplying it by 1 cm, the depth at which most zoospores are found. Suspensions of the various concentrations of zoospores were assigned randomly to each bucket within rows so that each treatment was duplicated per row and present in each row. The baiting process was identical to the one used in the field, and the number of infected bait leaves was recorded for each bucket at the end of a three-week study period.

Long-term field monitoring of inoculum pressure

The distribution of two vegetation types was identified in the Soquel Demonstration State Forest (Santa Cruz County, California, USA). The first, coded as L, included mixed evergreen stands with a dominance of California coast live oak (*Quercus agrifolia* Nee), bay, and Douglas-fir [*Pseudotsuga menziesii* (Mirb.) Franco]. The second, coded as LT, included "redwood–tanoak" stands where dominant tree species were redwoods, tanoaks, and bays. Four study plots within each vegetation type were chosen (Data S1). In all plots, the presence of SOD was confirmed by isolation of *P. ramorum* from symptomatic plant tissue, and all trees over 1 cm in diameter were mapped. Each plot was designed as a square with a side of 50 m, delimiting an ideal regular orthogonal grid formed by 10 × 10 m squared cells. A spore trap was placed on all inner nodes of the grid (i.e., excluding the ones along the plot border), totaling 16 buckets per plot (see Fig. 1) and

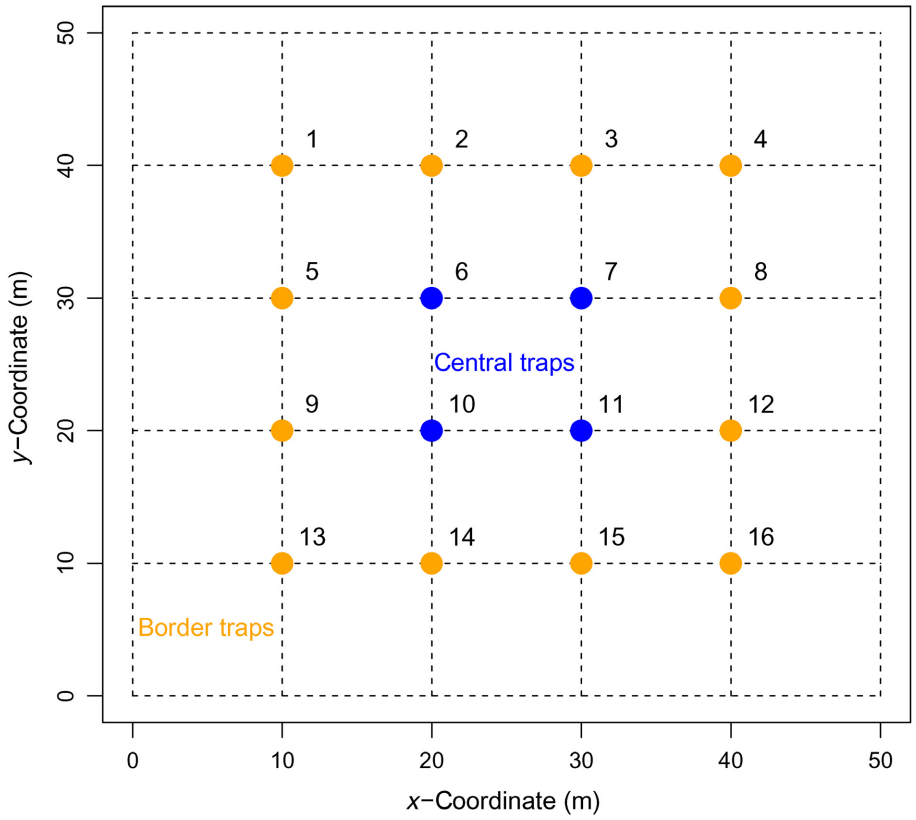

Fig. 1. Location of spore traps within plots. The dashed line delimits the orthogonal grid within the 50 × 50 m plots, with nodes every 10 m. Inner nodes host four central spore traps (blue points), while the outer nodes, excluding the ones along the border, contain the remaining 12 border traps (orange points). For treated plots, after bay removal, central traps and border traps are 20 and 10 m far, respectively, from the border of the no-bay area.

128 traps overall. Inoculum pressure of *P. ramorum* was quantified as described above for 7 yr. Monitoring was done at three-week intervals, all year long from February 2005 to December 2006 and from January to July in the 2007–2011 period. At the end of each monitoring interval, traps were coded as "red" events, when the inoculum pressure reached the threshold necessary for oak infection (i.e., four or five bait leaves were infected), while they were coded as "yellow" events when spore loads were below that threshold (i.e., less than four bait leaves were infected, see *Results*). No overflow or drying of the buckets were observed. Box-Pierce and Ljung-Box tests of independence were carried out on red events to check for serial correlation at lag 1 and lag 2, based on yearly and overall data (Box and Pierce 1970, Ljung and Box 1978, Crawley 2013).

Bay removal treatments and hotspot analysis

Two L and two LT plots were randomly assigned to be treatments (T plots), while the remaining four plots were assigned to be untreated controls (C plots). The treatment consisted in the complete eradication in September 2006 of all bays which were distributed within the T plots or whose canopies intersected their borders. Subsequently, the removal of bay resprouts was repeated once a year until the end of the experiment in 2011. Removal of all bays within T plots resulted in a no-bay buffer of 10 m for the 12 traps placed in the outer nodes of each grid (i.e., border traps), and in a no-bay buffer of 20 m for the four baiting buckets placed in the inner nodes (i.e., central traps; Fig. 1).

In order to determine the overall efficacy of the bay removal treatment, Fisher's exact tests were performed to compare the cumulated red events frequency between C and T plots on a yearly basis. The strength of the association between the treatments and the red events was assessed with the odds ratios and their exact 95% confidence intervals (95% CI) bounds, calculated with Fisher's method on the frequencies of red events cumulated for C and T plots, before and after treatment, respectively (Hosmer and Lemeshow 1989, Agresti 2001).

To determine whether a 20-m buffer is more effective than a 10-m buffer, yearly frequencies of red events were compared between central and border traps, separately for C and T plots. Additionally, we compared the cumulative yearly red frequencies found in central traps, between C and T plots, and the same comparison was made for the border traps. In all cases, frequencies comparisons were performed with the Fisher's exact test.

In order to test whether significant inoculum hotspots were present as points displaying large counts of red events, the cumulative absolute red events frequency was calculated per trap, within C plots, for the whole duration of the study. A Monte Carlo approximation of the exact χ^2 test, based on 2000 iterations, was carried out at the individual plot scale by comparing the observed red events frequencies with the frequencies expected under the assumption that red events were equally likely in all traps (i.e., under the null hypothesis of hotspots absence; Agresti 2001). The left-tailed Wald-Wolfowitz runs test (Wolfowitz 1943, Lewis 2013) was performed on the succession of red events displayed by those traps whose cumulative absolute frequency of such events was at least four (i.e., here defined as hotspots).

Relation between climatic variables and inoculum pressure

Daily average temperature (°C) and total rainfalls (mm; i.e., climatic variables) were measured at the meteorological station located in the Soquel Demonstration Forest (37°04′29.5″ latitude, −121°55′32.9″ longitude).

The frequency of positive traps (i.e., traps showing the presence of *P. ramorum* inoculum) and the average of the cumulative daily rainfalls were calculated for the semesters January–June and July–December, for all plots in 2005 and for C plots in 2006. The frequencies and the averages described above were compared between semesters of the same year with a Fisher's exact test and with a Mann-Whitney test, respectively.

A series of single-predictor binary logistic regressions was fit to model the overall proportion of red events observed in C plots, at each sampling performed in January–June from 2005 to 2011, as a function of the cumulative rainfalls calculated for the 7, 14, 21, and 30 d before samplings (r_7, r_{14}, r_{21}, and r_{30}, see Data S2: Sheet 1; Hosmer and Lemeshow 1989). The models were defined as M_{r7}, M_{r14}, M_{r21}, and M_{r30} depending on which cumulative rainfall variable was used as predictor, while the null model was referred as M_{r0} (Crawley 2013). For each model, the odds

ratios and the 95% CI associated with the intercept (β_0) and the single-predictor coefficient (β_1) were calculated. Significance of the regression coefficients was assessed with the Wald test, while models' comparison was made according to the minimum Akaike Information Criterion (AIC; Akaike 1973, Hosmer and Lemeshow 1989, Crawley 2013). Since no significant models were obtained (see *Results*), a bivariate Granger-causality test was performed between the same variables used to fit the binary logistic regressions after rank transformation (Granger 1969, Conover and Iman 1981, Hesse et al. 2003, Cacuci et al. 2005). The direction of the information transfer was set from the climatic variable to the red events frequency and the reliability of results was checked by inverting the direction of the information transfer. The optimal lag λ, from 1 to 10, was assessed based on the minimum AIC detected among the significant bivariate Granger-causality tests (Granger 1969, Akaike 1973, Conover and Iman 1981, Hesse et al. 2003, Balcombe 2005, Cacuci et al. 2005), and a Spearman's correlation analysis was performed between the λ-lagged values of the above rainfalls values and red events frequencies. The average of the cumulative rainfalls measured up to λ-lagged samplings before the occurrence of at least one red event was calculated along with the corresponding 95% normal bootstrap confidence interval.

In addition, binary logistic regression models were performed as described for rainfall, using average temperature values recorded in 7, 14, 21, and 30 d before sampling (t_7, t_{14}, t_{21}, and t_{30}, see Data S2: Sheet 1), resulting in models M_{t7}, M_{t14}, M_{t21}, and M_{t30} along with the null model M_{t0}. When temperature data were missing, the temperature of the nearest available timeframe was used. The means of the average temperature during the 7, 14, and 30 d (see *Results*) before the occurrence of at least one red event were calculated along with their corresponding 95% normal bootstrap confidence interval.

Tree species composition and inoculum pressure

To compare inoculum pressure of *P. ramorum* between the oak–bay mixed evergreen and the tanoak–redwood forests, cumulated red events frequencies were compared between L and LT plots with Fisher's exact tests. Values from all plots were used for the 2005–2006 baseline period (i.e., before treatments), while only values from C plots were used for the 2006–2011 period, after bays were removed from T plots.

To determine whether ecological interactions among tanoak and bays may affect sporulation, a geographic information system (GIS) based analysis was performed to assess the relationship between density of bays and of tanoaks in LT plots before treatments. Coordinates of bay and tanoak trees were customized assuming the southeastern vertex of each LT area as the origin of a Cartesian window whose axes were bound in the range 0–50 m (Data S3). The local density estimate of the two species was calculated with a Gaussian kernel method, with a bandwidth parameter set as described in Silverman (1986). For each species, density values were stored in a squared matrix corresponding to a raster image of 128 × 128 pixels (i.e., pixel edges corresponding to 39.06 cm, see Data S2: Sheets 2–9). Bay and tanoak density matrices were represented through heatmaps to assess their putative association, which was then analyzed with an element-wise Spearman's correlation carried out separately for each study plot.

A further investigation was performed to test whether bay density may be driving the frequency of red events. In all C plots, the local density of bays was calculated with the same kernel method described above. Three circular buffers were delimited around each trap, with a radius set at 1, 2.5, or 5 m. The average value of pixels indicating the local bay density was calculated for each circular buffer (Data S2: Sheet 10). The cumulative red events frequency of the whole sampling period was calculated for each trap. Binary logistic regression models were fitted for each plot using the proportion of red events as response variable, and the bay laurel average density associated with the circular buffer as predictor. Plot LT1C was excluded because the red events frequency was constant. Separate models were fitted for each buffer radius (i.e., M_1, $M_{2.5}$, and M_5 are associated with 1, 2.5, and 5 m radius buffer, respectively), along with the null model (i.e., M_0).

All statistical analyses were performed in R 3.2.3 (R Core Team 2015) with a significance threshold set to 0.05. The list of R libraries and functions used to perform the statistical tests is provided as Data S2: Sheet 11.

Results

Determination of inoculum pressure necessary to infect oaks and calibration of the baiting assay

In both oak inoculation trials, infection was successful only when using inoculum with concentration of 10^5 zoospores mL^{-1}. Average stem lesion size values (Data S2: Sheet 12) with associated standard error (±SE) when using the highest concentrations of zoospores were 161.51 ± 39.33 mm^2 and 301.33 ± 20.44 mm^2, in the first and second trial, respectively. Lesion size average values for inoculations using water and for inoculations using 10^3 and 10^4 zoospores mL^{-1} attained 9.58 ± 0.86, 11.19 ± 0.70, and 9.82 ± 0.27, and 10.97 ± 0.41, 11.78 ± 0.53, and 24.20 ± 8.70 (mm^2 ± SE) in the first and second trial, respectively. ANOVA and multiple comparisons analysis using Tukey's test showed that for both trials only lesions obtained with 10^5 zoospores mL^{-1} were significantly different from stem lesions obtained with all other treatments ($P < 0.01$ in both trials). Additionally, and in both trials, stem lesions using less than 10^5 zoospores/mL of solution as inoculum were not significantly different from those obtained by mock inoculations performed using only water ($P > 0.05$).

The three calibration trials performed to match baiting results with zoospore concentration showed that in 98.2% of replicates the number of bait leaves with *Phytophthora ramorum* leaf lesions was three or less per bucket when zoospore concentration was 10^4 mL^{-1} or less. Conversely, when zoospore concentration was above 10^4 mL^{-1}, in 91.0% of replicates four or five bait leaves were infected (Data S2: Sheet 13).

Consequently, results from the field sampling were partitioned in two: (1) When less than four leaves per trapping bucket were found to be infected, that event was coded as a "yellow," implying inoculum potential did not reach the threshold necessary for oak infection; (2) when four or five leaves in a trapping bucket were found to be infected, that event was coded as a "red," implying that inoculum had reached the threshold necessary to cause oak infection. The experiment generated close to 6450 lines of data (Data S2: Sheet 14). Box-Pierce and Ljung-Box tests agreed in excluding the presence of serial autocorrelation in red events, regardless of the lag considered ($P > 0.05$; Appendix S2: Table S1).

Bay removal treatments and hotspot analysis

Results of the long-term monitoring of inoculum pressure of *P. ramorum* showed that the yearly frequency of red events when spore loads were over the threshold necessary to infect the oaks ranged between 0% and 6.51%. Fisher's exact tests did not detect significant differences ($P > 0.05$) between C and T plots in 2005–2006, before the bay removal treatment was administered. The same result was observed during the first two years after the treatment (2007–2008) due to the fact the frequency of red events was constantly 0%, regardless of plot. However, starting from the third year after treatment, and until the end of the experiment (2009–2010–2011), red events frequency was significantly lower ($P < 0.05$) in T than in C plots (Fig. 2). Before bay removal was performed, a 0.30 non-significant odds ratio was obtained (95% CI: 0.07–1.04). However, after treatment, the odds ratio decreased to 0.15 (95% CI: 0.07–0.30), indicating a significant and negative association between treatment and the frequency of red events.

When the same analyses were performed comparing frequencies of red events between central and border traps, separately for C (Appendix S1: Fig. S2) and T (Appendix S1: Fig. S3) plots, no statistical differences were found ($P > 0.05$). However, comparisons between C and T plots of the yearly cumulated red events frequencies in central traps and in border traps showed that, after treatment, significantly lower values ($P < 0.05$) were displayed more frequently by central traps (2009–2011) than by border ones (only 2009; Table 1).

Results of the Monte Carlo approximation of the exact χ^2 test showed that in the two L control plots (i.e., mixed evergreen stands) the observed frequencies of the red events were significantly different from the frequencies expected under the null hypothesis of hotspots absence ($P < 0.05$), while in the two LT control plots (i.e., redwood–tanoak stands) such difference was not detected ($P > 0.05$; Appendix S2: Table S2). Seven hotspots were detected, with a total cumulative absolute frequency of red events comprised between four and nine. The Wald-Wolfowitz test was significant for two out of seven hotspots ($P < 0.05$), indicating an under-mixing of runs, while for the other hotspots the runs showed a randomized pattern ($P > 0.05$; Appendix S2: Table S3).

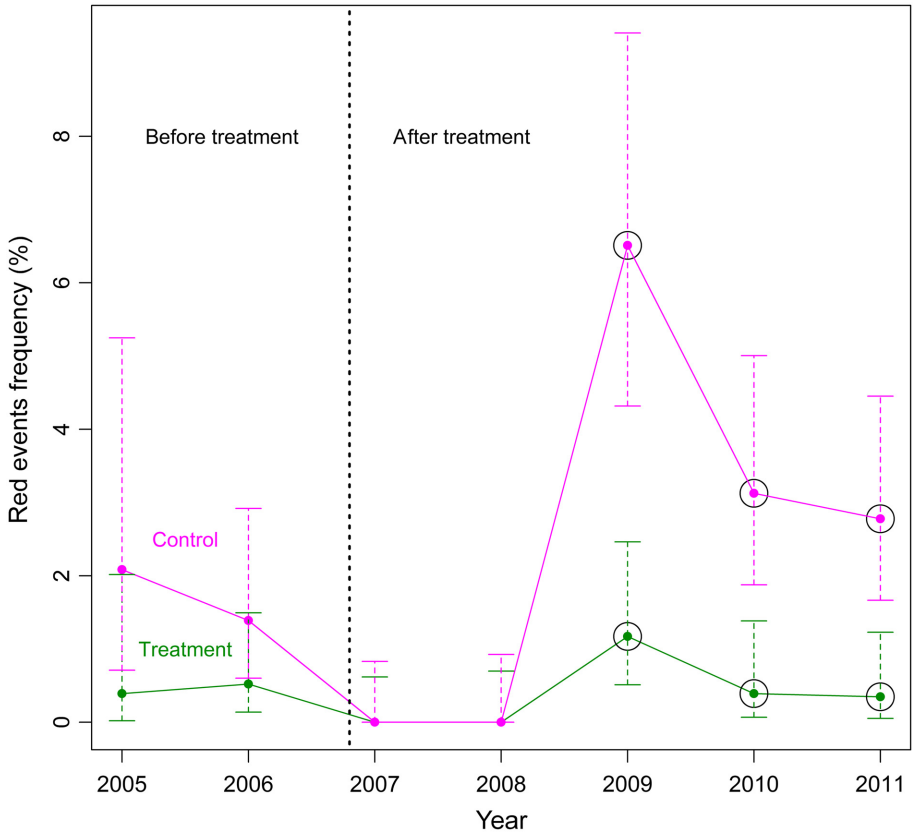

Fig. 2. Assessment of the efficacy of the bay removal treatment. Comparison of frequency (%) of events when inoculum loads were high enough to infect oaks (red events) between control (C-magenta line) and treated (T-green line) plots for each sampling year. Circled values indicate significance at 0.05 level according to the results of the Fisher's exact test. The dotted line represents the treatment time. Error bars refer to 95% exact confidence intervals.

Table 1. Comparison of the cumulated yearly red events frequency between treated and control plots in central and border traps.

	Comparison of red events frequency (%) in central traps			Comparison of red events frequency (%) in border traps		
Sampling year	Treatment (T)	Control (C)	*P*-value	Treatment (T)	Control (C)	*P*-value
2005	0.00	0.00	1.00	0.52	2.78	0.17
2006	0.00	0.93	0.43	0.69	1.54	0.30
2007	0.00	0.00	1.00	0.00	0.00	1.00
2008	0.00	0.00	1.00	0.00	0.00	1.00
2009	0.78	8.33	0.01*	1.30	5.90	0.00*
2010	0.00	5.47	0.01*	0.52	2.34	0.06
2011	0.00	4.86	0.01*	0.46	2.08	0.06

Notes: For each sampling year, the cumulated red events frequencies (in %) of the central traps and of the border traps are compared between treated (T) and control (C) plots with the Fisher's exact test, whose *P*-values are reported. Asterisks indicate significant ($P < 0.05$) comparisons. Graphs derived from this table, including 95% confidence intervals, are available in Appendix S1: Figs. S2 and S3.

Table 2. Binary logistic regressions modeling the proportion of events when inoculum loads were high enough to infect oaks (red events) as a function of the cumulative rainfalls measured before samplings in control plots.

Model	AIC	Coefficient	*P*	95% CI	Odds ratio
M_{r0}	256.19	$\beta_0 = -3.75^*$	$<1 \times 10^{-15}$	−4.00; −3.52	2.35×10^{-2}
M_{r7}	254.54	$\beta_0 = -3.61^*$	$<1 \times 10^{-15}$	−3.89; −3.34	2.71×10^{-2}
		$\beta_1 = -7.86 \times 10^{-3}$	0.08	-1.78×10^{-2}; 1.82×10^{-4}	0.992
M_{r14}	257.06	$\beta_0 = -3.66^*$	$<1 \times 10^{-15}$	−3.96; −.39	2.56×10^{-2}
		$\beta_1 = -1.88 \times 10^{-3}$	0.31	-5.89×10^{-3}; 1.47×10^{-3}	0.998
M_{r21}	258.04	$\beta_0 = -3.71^*$	$<1 \times 10^{-15}$	−4.03; −3.41	2.44×10^{-2}
		$\beta_1 = -4.80 \times 10^{-4}$	0.71	-3.16×10^{-3}; 1.90×10^{-3}	0.999
M_{r30}	256.45	$\beta_0 = -3.60^*$	$<1 \times 10^{-15}$	−3.93; −3.29	2.73×10^{-2}
		$\beta_1 = -1.43 \times 10^{-3}$	0.21	-3.78×10^{-3}; 6.58×10^{-4}	0.999

Notes: β coefficients (β_0 for the intercept, β_1 for the predictor), their related *P*-values, 95% confidence intervals (CI), odds ratios, and the Akaike Information Criterion (AIC) are reported for each model. Asterisks indicate significant ($P < 0.05$) coefficients. Models acronyms refer to the null model (M_{r0}) and to the models whose predictors were the cumulative rainfalls of the 7, 14, 21, and 30 d before samplings (M_{r7}, M_{r14}, M_{r21}, and M_{r30}, respectively).

Effect of climate on sporulation levels

When comparing frequency of positive traps in the first two years of the experiment in all plots, the percentage of positive traps was significantly lower in the July–December period than in the January–June period (0.78% vs. 10.16% in 2005, 0.19% vs. 5.38% in 2006; $P < 0.05$). Additionally, the average of the cumulative daily rainfalls differed significantly between the two semesters, with the July–December period being drier than the January–June one (3.18 vs. 4.26 mm in 2005, 1.28 vs. 4.64 mm in 2006, $P < 0.05$).

No significant β_1 coefficients ($P < 0.05$) were displayed by binary logistic regressions M_{r7}, M_{r14}, M_{r21}, and M_{r30} modeling the proportion of red events as a function of the cumulative rainfalls measured before samplings. The β_1 95% CI, displaying lower and upper bounds with opposite sign, and the odds ratios, not substantially different from 1, confirmed the absence of association between the predictor and the probability associated with red events. Accordingly, the AIC values associated with those models, ranging from 254.54 to 256.45, were not substantially different from the M_{r0} AIC that attained a value of 256.19 (Table 2). Instead, up to five significant tests per rainfall ($P < 0.05$) were obtained with the bivariate Granger-causality analysis performed between the lagged values of the r_7, r_{14}, r_{21}, and r_{30} and the proportion of red events, with the information transfer direction set from the climatic variables to the red events frequency. For all rainfall variables, the minimum AIC among significant tests indicated $\lambda = 2$ as optimal lag (Table 3). No significant results were obtained when the information transfer direction was inverted, confirming the reliability of the Granger-causality results. Positive correlations were observed between all two-lagged rainfall variables and the red events frequencies, with Spearman's ρ values of 0.30 ($P > 0.05$) for r_7, 0.48 ($P < 0.05$) for r_{14}, 0.32 ($P < 0.05$) for r_{21}, and 0.37 ($P < 0.05$) for r_{30}, respectively. The average of the cumulative rainfalls measured up to two-lagged samplings before the occurrence of at least one red event attained 248 mm (171–324 95% CI).

In the M_{t7}, M_{t14}, and M_{t30} equations modeling the proportion of red events as a function of the average temperatures measured before samplings, significant and positive β_1 coefficients ($P < 0.05$) were obtained, while the null hypothesis could not be rejected ($P > 0.05$) for the β_1 resulting from M_{t21}. Models with significant β_1 had AIC values comprising between 229.28 and 238.99, lower than the AIC values achieved by M_{t0} and M_{t21}, which were substantially similar (240.79 and 240.22). In models M_{t7}, M_{t14}, and M_{t30}, the lower and upper bounds of the β_1 coefficient displayed a positive sign, with a related odds ratio higher than 1, showing that increasing temperatures are associated with raising probability of red events to occur. Although in M_{t21} the odds ratio related to β_1 attained 1.05, the opposite signs of the 95% CI lower and upper bounds confirmed that the association between t_{21} and the above probability was not significant (Table 4). Mean average temperatures were 11.9°C (10.0–13.8 95% CI), 10.9°C (9.2–12.6 95% CI), and 10.4°C

Table 3. Bivariate Granger-causality analysis performed between the lagged values of cumulative rainfalls measured before samplings and the proportion of events when inoculum loads were high enough to infect oaks (red events).

λ	Statistics	r_7	r_{14}	r_{21}	r_{30}
1	*F*	4.26*	2.29	1.25	3.02
	P-value	0.04	0.14	0.27	0.09
	AIC	11.98	11.88	11.62	11.57
2	*F*	3.67*	7.87*	3.75*	5.24*
	P-value	0.03	1.11×10^{-3}	0.03	0.01
	AIC	11.88**	11.58**	11.47**	11.32**
3	*F*	2.29	5.27*	2.33	3.22*
	P-value	0.09	3.35×10^{-3}	0.09	0.03
	AIC	12.02	11.66	11.58	11.41
4	*F*	1.59	3.67*	1.68	2.20
	P-value	0.19	0.01	0.17	0.08
	AIC	12.04	11.78	11.72	11.48
5	*F*	1.82	3.58*	1.68	2.26
	P-value	0.13	0.01	0.16	0.07
	AIC	12.15	11.85	11.66	11.28
6	*F*	1.41	3.10*	2.09	1.78
	P-value	0.24	0.01	0.08	0.13
	AIC	12.21	11.79	11.62	11.40
7	*F*	0.76	1.93	1.17	1.15
	P-value	0.62	0.10	0.34	0.36
	AIC	12.11	11.74	11.44	11.26
8	*F*	0.70	1.84	1.09	1.02
	P-value	0.69	0.11	0.40	0.44
	AIC	12.15	11.81	11.59	11.33
9	*F*	0.68	1.56	1.18	1.05
	P-value	0.72	0.18	0.34	0.43
	AIC	12.08	11.87	11.48	11.11
10	*F*	0.57	1.26	1.32	0.95
	P-value	0.82	0.30	0.28	0.51
	AIC	12.22	12.00	11.53	11.22

Notes: The Granger *F* statistic, its related *P*-value, and the corresponding Akaike Information Criterion (AIC) are indicated for each lag λ and rainfall variable, namely the cumulative rainfalls of the 7, 14, 21, and 30 d before samplings (r_7, r_{14}, r_{21}, and r_{30}, respectively). The single asterisk marks significant ($P < 0.05$) Granger *F* values, while the double asterisk highlights the minimum AIC among the significant tests.

(8.9–11.8 95% CI), during the 7, 14, and 30 d before the occurrence of at least one red event (i.e., corresponding to the above significant β_1 coefficients), respectively.

The graphical representation of the climatic variables that were analyzed confirmed the presence of a positive, but lagged, effect of rainfall values, and a positive, not-lagged effect of temperature values on the probability of observing a red event (Fig. 3).

Tree species composition and inoculum pressure

When comparing the frequency of red events between mixed evergreen (L) and tanoak–redwood (LT) plots, values were significantly higher in the first than in the second. This was true both when comparing all study sites before bay removal (2.48% vs. 1.13%; $P < 0.05$) and when comparing the entire dataset for control plots (C) only (3.41% vs. 0.61%; $P < 0.05$).

To determine the effect of the ecological interaction between bay and tanoak on red events, a kernel density analysis was performed. Kernel methods for the estimation of density are statistical tools mainly used for the estimation of probability density curves (Silverman 1986), but they have also been used to investigate ecological phenomena (see Worton 1989, Nelson and Boots 2008) and to validate results of genetic structure analyses (Garbelotto et al. 2013). Heatmaps showing estimated bay and tanoak densities using the kernel method suggested an inverse association between the two underlying matrices (Appendix S1: Fig. S4). The negative association between bay and tanoak density was confirmed by a Spearman's correlation analysis, showing negative and significant coefficients in three plots ($\rho = -0.80$, $\rho = -0.47$, $\rho = -0.46$, $P < 0.05$) and a negative, yet not significant coefficient in the last one ($\rho = -0.01$, $P > 0.05$).

The fit of binary logistic regression equations expressing the proportion of red events as a function of the bay laurel average density associated with each circular buffer resulted in positive and significant ($P < 0.05$) β_1 coefficients for all buffer radii in two out of three plots. The association between increasing bay laurel density and higher probability of red events was confirmed by the β_1 95% CI, excluding 0, as well as by the odds ratio displaying values substantially larger than 1. In the remaining plot, the β_1 coefficient was positive, but not significant ($P > 0.05$), and its associated 95% CI was characterized by bounds with opposite sign, excluding the significance of the association between predictor and dependent variable, despite the large value of the odds ratio (Table 5).

Discussion

The main focus of the research reported here was to identify and define the epidemiological,

Table 4. Binary logistic regressions modeling the proportion of events when inoculum loads were high enough to infect oaks (red events) as a function of the average temperatures measured before samplings in control plots.

Model	AIC	Coefficient	*P*	95% CI	Odds ratio
M_{t0}	240.79	$\beta_0 = -3.70^*$	$<1 \times 10^{-15}$	−3.96; −3.46	2.46×10^{-2}
M_{t7}	229.28	$\beta_0 = -4.96^*$	$<1 \times 10^{-15}$	−5.78; −4.22	6.98×10^{-3}
		$\beta_1 = 9.81 \times 10^{-2*}$	2.78×10^{-4}	4.57×10^{-2}; 1.52×10^{-1}	1.10
M_{t14}	236.92	$\beta_0 = -4.57^*$	$<1 \times 10^{-15}$	−5.37; −3.82	1.04×10^{-2}
		$\beta_1 = 7.27 \times 10^{-2*}$	2.00×10^{-2}	1.39×10^{-2}; 1.32×10^{-1}	1.07
M_{t21}	240.22	$\beta_0 = -4.28^*$	$<1 \times 10^{-15}$	−5.08; −3.54	1.38×10^{-2}
		$\beta_1 = 5.12 \times 10^{-2}$	1.10×10^{-1}	-1.15×10^{-2}; 1.13×10^{-1}	1.05
M_{t30}	238.99	$\beta_0 = -4.42^*$	$<1 \times 10^{-15}$	−5.24; −3.66	1.20×10^{-2}
		$\beta_1 = 6.51 \times 10^{-2*}$	4.94×10^{-2}	3.46×10^{-4}; 1.30×10^{-1}	1.07

Notes: β coefficients (β_0 for the intercept, β_1 for the predictor), their related *P*-values, 95% confidence intervals (CI), odds ratios, and the Akaike Information Criterion (AIC) are reported for each model. Asterisks indicate significant ($P < 0.05$) coefficients. Models acronyms refer to the null model (M_{t0}) and to the models whose predictors were the average temperatures of the 7, 14, 21, and 30 d before samplings (M_{t7}, M_{t14}, M_{t21}, and M_{t30}, respectively).

climatic, and ecological parameters driving infection of oaks by the SOD pathogen *Phytophthora ramorum*. The analyses presented hinge on the determination of the inoculum threshold necessary to infect coast live oaks, and on a long-term monitoring of such inoculum levels in a forest setting. A series of analyses were performed to assess and quantify the association between high inoculum levels and a variety of stand and climatic variables. Our results are among the first to define several disease transmission metrics for a dead-end plant host, and thus provide a general term of comparison for other plant and animal diseases and for the study of landscape-level effects on the dispersal of plant pathogens (Plantegenest et al. 2007). In fact, such studies in forest settings are notably few (Holdenrieder et al. 2004).

For diseases whose contagion is mediated by a vector, there is a substantial difference whether that vector is an insect or a transmissive host. Although many plant diseases are vectored by insects (Gilbert 2007), the category of plant diseases for which the pathogen is transmitted from a transmissive or reservoir host to a dead-end host plant includes a limited number of cases and SOD, in its narrower definition of an infectious disease causing mortality of true oaks, may be one of the few known cases falling precisely into this category. In fact, *P. ramorum* stands among the few plant pathogens, at least among oomycetes and fungi, causing such severe symptoms to hosts (i.e., oaks) that it cannot sporulate on. Manipulative and descriptive infection studies have determined that (1) infection of oaks is about one order of magnitude less frequent than that of tanoaks in artificial inoculations of adult trees in nature (Davidson et al. 2005, McPherson et al. 2010); (2) larger oaks are more likely to be infected (McPherson et al. 2010); (3) most infected oaks lie within 10 m from a bay (Kelly and Meentemeyer 2002, Liu et al. 2007, Swiecki and Bernhardt 2008); and (4) bays are the most infectious hosts in nature (Davidson et al. 2005). More in-depth analyses of oak infection are missing and most studies so far attempting to model the disease have rather focused on aspects such as climate and general host community composition (Meentemeyer et al. 2004, 2008, 2011, 2015).

Several studies have corroborated the notion that bay laurels act as transmissive hosts of SOD to oaks. For instance, population studies demonstrated that bay leaves harbor a few dominant genotypes, which are persistent through time (Mascheretti et al. 2009), precisely as expected when the host is epidemiologically relevant (Eyre et al. 2013). In most infectious diseases, including SOD, infectious outbreaks are caused by highly transmissive genotypes or strains that are overly represented when compared to other genotypes (Berbegal et al. 2013, Gramaje et al. 2014, Sillo et al. 2017). On the contrary, in substrates with nil or negligible epidemiological role, either a high turnover of genotypes occurs (e.g., in water and soil), or genetic structural variations causing a significant change in phenotype can be observed (e.g., in oaks; Eyre et al. 2013, 2014). Moreover, no genetic structure has been recorded when

comparing populations from oaks and those from bays (Kasuga et al. 2012).

Differently from vector-borne contagion, airborne spores must reach the dead-end host in numbers or densities sufficient to successfully infect that host. It is worth noting that most infected oaks grow within 10 m from bay laurels, while infected bays or tanoaks can be detected at hundreds of meters from the closest source of infection. This seems to point out that the threshold of sporangia necessary for oak infection is significantly higher than the one needed to infect bays or tanoaks. This observation is in agreement with the lack of correlation between infected oaks and tanoaks; in fact, tanoaks are also known to be transmissive hosts, but with a distinctively lower inoculum potential than bay laurels (Davidson et al. 2005). Our inoculation experiments showed that oak infection occurs only if the zoospore concentration per ml is over the threshold of 10^4, that is, two to three orders of magnitude higher than the threshold required for foliar infections of other hosts (Hüberli et al. 2008, Eyre et al. 2014).

Two prerequisites may be necessary to reach such threshold: (1) proximity to bay laurels as the only likely source of high levels of inoculum and (2) presence of weather conditions conducive to high sporulation levels. Our results confirmed that high levels of inoculum are not frequently reached throughout the landscape, but tend to occur in specific locations. In fact, in 55 samplings collected over seven years of monitoring across 128 points split into two forest types, the incidence of high levels of inoculum reached a maximum frequency of ~6.51% on a yearly basis and only in some of the study plots. It is worth noting that the incidence of red events is unlikely to have been biased by the repeated assessment of the inoculum loads in the same plots. In fact, while such design could theoretically expose to the risk of temporal pseudoreplication, the tests carried out to check for serial correlation excluded this possibility, hence justifying the statistical approach here proposed (e.g., analyses on cumulated red events frequencies) (Box and Pierce 1970, Ljung and Box 1978, Crawley 2013). Moreover, a large amount of our results was derived from robust statistical methods (e.g., Fisher's exact tests), based on permutation approaches, whose validity in providing reliable outcomes, regardless of the sampling size, has been largely documented (Agresti 2001, Carsey and Harden 2014, Lione and Gonthier 2016).

Our models show that high thresholds necessary for oak infection are more likely to occur in association with a high density of bay laurels within 5 m from traps collecting sporangia, and only in correlation with abundant rainfalls prior to the sampling period and with warmer temperatures during the sampling period.

The effect of rainfall in promoting the production of high amounts of inoculum is not immediate; otherwise, binary regression coefficients for rainfall values should have been significant. Nonetheless, the mere observation of the climatic graph depicting the occurrence of rainfalls along with episodes of high inoculum pressure suggested that rainfall may exert an effect on sporulation, but with delay. The Granger-causality analysis allowed the assessment of such a delay, corresponding to a shift of two samplings, equivalent to a timeframe of ~6 weeks. Such a delay corresponds to an average input of cumulative rainfalls of 248 mm, which could be deemed as an alert threshold to suspect likely oak infections. Noteworthily, the outcomes of the Granger-causality analysis supported the results gathered from the Box-Pierce and Ljung-Box tests, showing that the autoregressive component of the red events was completely negligible in comparison with the effect of the rainfalls (Granger 1969). Spearman's coefficients further confirmed the positive correlation between the magnitude of the water input and the inoculum pressure. The lagged effect of climatic parameters, such as rainfall, on the production of fungal inoculum and on the insurgence of the associated diseases is not a novelty, since it has been previously documented in the literature (Johnson 1994, Stennett and Beggs 2004, Ndoumbè-Nkeng et al. 2009, Yan et al. 2011). However, this is the first study reporting the association between rainfall and the amount of *P. ramorum* inoculum above the threshold required to infect oaks. From a biological point of view, the lagged effect of rainfalls is not surprising, since the pathogen population is likely to require a certain amount of time to achieve a sporulation potential able to reach and overcome such threshold. Average temperature was also identified as a variable positively correlated with increasing sporulation levels, as shown

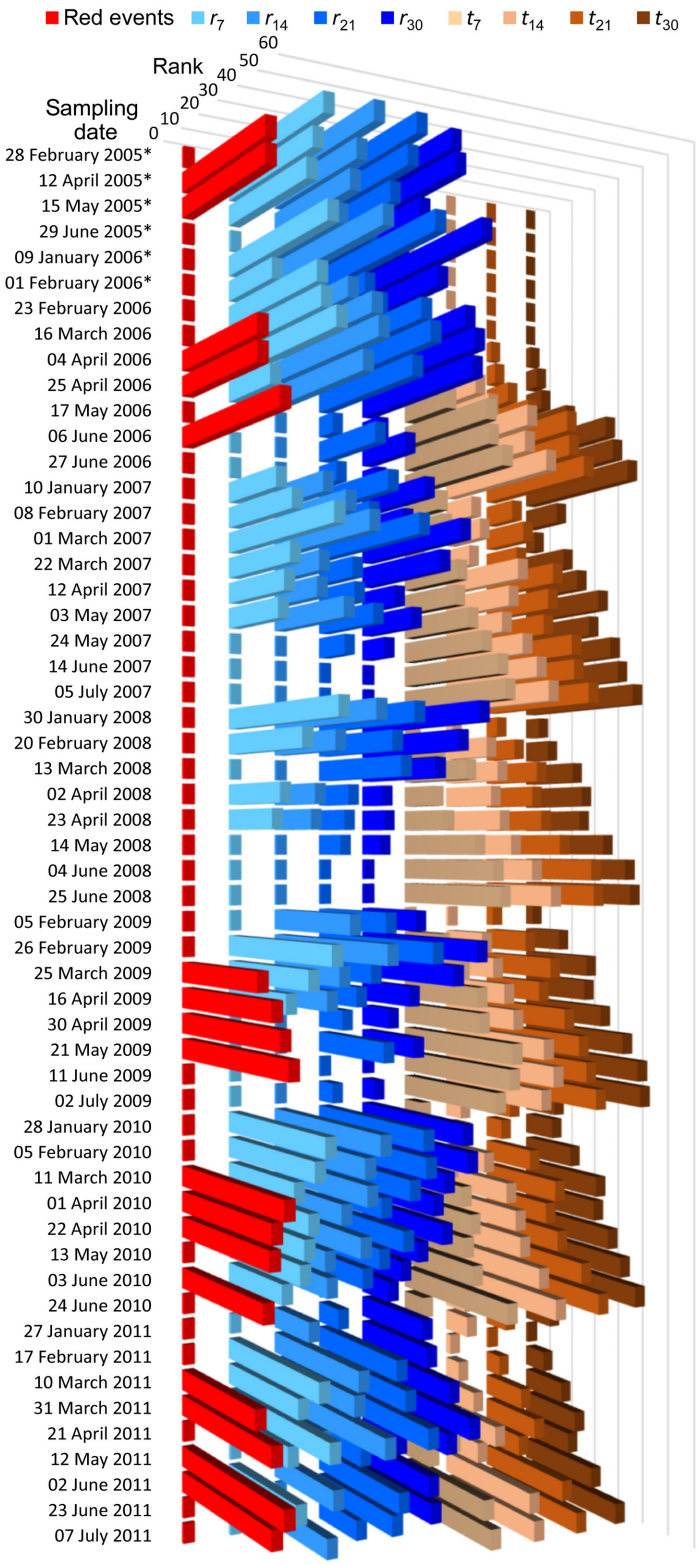

Fig. 3. Frequency of events when inoculum loads were high enough to infect oaks (red events), cumulative

(*Fig. 3. Continued*)
rainfalls, and average temperatures associated with each sampling. Climatic variables refer to the average temperatures (°C) and cumulative rainfalls (mm) of the 7, 14, 21, and 30 d before sampling (t_7, t_{14}, t_{21}, and t_{30} for temperatures and r_7, r_{14}, r_{21}, and r_{30} for rainfalls, respectively). For every sampling date, the ranked-transformed values of the red events frequencies, the cumulative rainfalls, and the average temperatures measured before samplings are reported. A lag from rainfall bars to red events bars is present, while no visible lags for temperature bars can be visually detected. Asterisks indicate missing values for temperatures.

by the corresponding binary logistic regressions. In particular, the values achieved by the odds ratios pointed out that temperature is a relevant risk factor, whose increasing values boost the probability of red events. It is worth noting that odds ratios are commonly used to investigate ecological associations in plant pathology, since their interpretation is immediate (i.e., positive, null, or negative associations with values higher than 1, equal to 1, or between 0 and 1, respectively; Hosmer and Lemeshow 1989, Gonthier et al. 2012, Lione et al. 2016). Odds ratio, 95% CI, and the significance of the average temperatures coefficients in the above logistic models indicated that the effect of temperature on sporulation may occur without the delay observed for rainfall; that is, a higher percentage of red events were scored when temperatures during the sampling period were warmer. On average, mean temperatures around 10.5°–12°C during a timeframe of 7–30 d might represent an alarm bell associated with increasing probability of observing oak infections. As a result, the majority of red events were recorded between March and May. It is worth noting that within the range of the average temperature measured during the sampling period (average minimum 4.23°C, average maximum 20.75°C), our results are consistent with in vitro growth and sporulation trials performed to assess the response of the pathogen to temperature (Englander et al.

Table 5. Binary logistic regressions modeling the proportion of events when inoculum loads were high enough to infect oaks (red events) as a function of the bay laurel average density.

Plot	Model	AIC	Coefficient	*P*	95% CI	Odds ratio
L1C	M_0	60.882	$\beta_0 = -3.76^*$	$<1 \times 10^{-15}$	−4.24; −3.35	2.33×10^{-2}
	M_1	48.979	$\beta_0 = -6.39^*$	$<1 \times 10^{-15}$	−8.03; −4.90	1.68×10^{-3}
			$\beta_1 = 143.77^*$	9.93×10^{-5}	70.07; 215.97	2.76×10^{62}
	$M_{2.5}$	48.939	$\beta_0 = -6.45^*$	$<1 \times 10^{-15}$	−8.11; −4.93	1.58×10^{-3}
			$\beta_1 = 146.98^*$	9.83×10^{-5}	71.71; 220.76	6.80×10^{63}
	M_5	48.893	$\beta_0 = -6.62^*$	$<1 \times 10^{-15}$	−8.37; −5.02	1.33×10^{-3}
			$\beta_1 = 155.75^*$	9.87×10^{-5}	76.05; 234.02	6.39×10^{67}
L2C	M_0	92.741	$\beta_0 = -3.04^*$	$<1 \times 10^{-15}$	−3.38; −2.74	4.76×10^{-2}
	M_1	84.856	$\beta_0 = -4.09^*$	$<1 \times 10^{-15}$	−4.92; −3.35	1.67×10^{-2}
			$\beta_1 = 37.47^*$	1.42×10^{-3}	14.30; 60.55	1.88×10^{16}
	$M_{2.5}$	84.807	$\beta_0 = -4.11^*$	$<1 \times 10^{-15}$	−4.94; −3.36	1.64×10^{-2}
			$\beta_1 = 38.24^*$	1.38×10^{-3}	14.65; 61.72	4.06×10^{16}
	M_5	84.789	$\beta_0 = -4.17^*$	$<1 \times 10^{-15}$	−5.04; −3.38	1.54×10^{-2}
			$\beta_1 = 41.01^*$	1.36×10^{-3}	15.74; 66.14	6.44×10^{17}
LT2C	M_0	28.941	$\beta_0 = -4.83^*$	$<1 \times 10^{-15}$	−5.67; −4.16	8.02×10^{-3}
	M_1	30.613	$\beta_0 = -5.24^*$	$<1 \times 10^{-10}$	−7.04; −3.69	5.67×10^{-3}
			$\beta_1 = 31.37$	0.55	−85.62; 128.39	4.19×10^{13}
	$M_{2.5}$	30.583	$\beta_0 = -5.27^*$	$<1 \times 10^{-10}$	−7.10; −3.69	5.13×10^{-3}
			$\beta_1 = 33.43$	0.54	−85.52; 132.76	3.31×10^{14}
	M_5	30.447	$\beta_0 = -5.39^*$	$<1 \times 10^{-9}$	−7.33; −3.72	4.57×10^{-3}
			$\beta_1 = 42.21$	0.47	−83.73; 150.25	2.15×10^{18}

Notes: β coefficients (β_0 for the intercept, β_1 for the predictor), their related *P*-values, 95% confidence intervals (CI), odds ratios, and the Akaike Information Criterion (AIC) are reported for each model. Asterisks indicate significant ($P < 0.05$) coefficients. Models acronyms refer to the null model (M_0) and to the models whose predictors were the 1-, 2.5-, and 5-m circular buffers (M_1, $M_{2.5}$, and M_5, respectively).

2006). These comparisons are often pivotal to assess the consistency between climatic models outcomes and pathogens' biology (Lione et al. 2015). A further confirmation of the pivotal role played by rainfall in determining high sporulation levels may be gathered from the observation that inoculum thresholds necessary for oak infections were never reached in the dry 2007 and 2008 yr, when rainfall values were merely 498 and 847 mm against an average of 1116 mm. One of the implications of these results is that oak infection may only occur in years with abundant rainfall and not on a yearly basis. Additionally, even considering wet years, oak infection may occur only between March and May, when warm temperatures intersect abundant rainfall. Although rain events in the fall may be accompanied by warm temperatures, they are probably too short to exert a substantial effect on sporulation, especially considering that a six-week delay is needed to reach those effects. While several studies have determined a positive relationship between rainfall and SOD levels (Davidson et al. 2005, 2008, Meentemeyer et al. 2008, 2015, Eyre et al. 2013), this is the first study to analyze the relationship between climatic variables and inoculum levels high enough to cause bay-to-oak disease transmission. These results allow for the first time to precisely determine when and how frequently oak infection may occur, a piece of information bound to be pivotal when modeling oak mortality caused by SOD.

Sites in the mixed evergreen forest displayed a higher incidence of high sporulation events, once again confirming bay laurels are the source of infection for oaks. The presence of tanoak, another well-known infectious host (Garbelotto et al. 2003, Davidson et al. 2005), did not act synergistically with bay on sporulation levels. Quite the contrary, our kernel density analysis showed that increasing density of tanoak resulted in lower density of bay, indicating a clear ecological antagonism between the two species. Because tanoaks are known to support *P. ramorum* sporulation less than bays (Garbelotto et al. 2003, Davidson et al. 2005), this result explains why sites with the presence of both hosts were characterized by lower levels of inoculum. This finding suggests an inoculum dilution effect caused by higher host diversity, resulting in lower transmission levels (Keesing et al. 2006). Other studies have suggested that high host diversity may reduce SOD outbreaks, but have failed to identify dilution as the most likely mechanism of such reduction. In mixed evergreen sites, where bays were abundant, hotspots of events displaying oak-infectious inoculum pressure were detected, while no hotspots could be identified where both tanoaks and bays were present, once again suggesting that such events may be rarer and not predictable as the density of bays decreases. We conclude that the role played by tanoaks, and by other hosts for that matter, may be negligible in oak infection. We also conclude that any host in ecological competition with bay laurels may reduce the severity of outbreaks of oak mortality caused by SOD.

Once ascertained the primary role played by bay in generating high inoculum pressure, the next step consisted in quantifying the relationship between bay density and the occurrence of high inoculum levels. Our results showed a strong and positive correlation between high inoculum levels and density of bays within buffers up to 10 m in diameter. Results also showed that hotspots of high inoculum levels could be found across a forested landscape, but only associated with bay, once again supporting the concept of a strong relation between the abundance of bays and high inoculum levels. Thus, it is relevant, but not surprising, that we were able to significantly lower the incidence of high *P. ramorum* inoculum events by removing bays for distances of either 10 or 20 m from our survey points. These distances are also in agreement with data published in previous studies (Kelly and Meentemeyer 2002, Liu et al. 2007). Bay removal is an effective, feasible, cost-effective operation, and as such, it may provide an invaluable disease management tool. Our results showed not only the efficacy of the removal treatment, but also that a removal buffer of 10 m was sufficient to drastically reduce the number of events in which inoculum pressure was high enough to infect oaks. This effect was independent of the presence or absence of tanoaks. Despite its effectiveness, bay laurel removal might be unpractical as a large-scale management tool for obvious reasons, yet it can exert all its potential in the preservation of limited forest patches, urban parks, or private gardens where the protection of oak is deemed pivotal. Such cases may encompass areas of particular aesthetic, ornamental, naturalistic, or recreational value, as well as situations where

landscape conservation is a priority. This approach is fully consistent with forest management policies suggested to control other alien invasive pathogens (e.g., *Heterobasidion irregulare* Garbelotto & Otrosina in Europe), whose main core relies in the selection of areas and objectives ranked according to different priorities (Gonthier et al. 2014).

A comparison of frequency of red events between control and treatment plots suggested that 20-m no-bay buffers may further reduce the likelihood of encountering oak-infectious inoculum levels. It has been reported that larger oaks are more likely to become infected (McPherson et al. 2010); hence, we suggest that a no-bay buffer up to 20 m may be beneficial for larger trees. Of course, we cannot exclude that in the presence of rainfall values significantly greater than those experienced during the course of the study, the effect of bay removal limited to 10–20 m may be less marked. It has been shown that oaks treated with phosphites display a reduced susceptibility to *P. ramorum* (Garbelotto et al. 2009). Such practice may thus extend the efficacy of spatially defined bay removal to all weather conditions, within a framework of a combined control strategies acting both on the reservoir (bay removal) and on the dead-end host (increasing the inoculum levels necessary for successful infection).

One notable unique finding of this study has been the almost absolute lack of measurable sporulation in dry but foggy periods. This is quite surprising due to the high values of leaf wetness observed in coastal forests in association with heavy fog (Dawson 1998). However, this could be related to ecological factors involved in epidemiological dynamics. Leaf wetness observed during foggy period might not provide a film of water endowed with suitable characteristics in terms of thickness and continuity. The fact that sporulation is strictly linked to rainfall might be an adaptive trait for a pathogen that can only complete its infection process through a persistent film of water. The connection with rainfall also confirms that spread of *P. ramorum* is splash-mediated, as it has been reported for other *Phytophthora* species and notably *P. capsici* (Ristaino and Gumpertz 2000). Splash dispersal is regulated by both the size of the propagule and the size of the droplet. Windborne droplets may be responsible for longer-distance dispersal; however, the vast majority of splash dispersal occurs in the range of a few meters, while dispersal in the tens of meters may be effected only at low concentrations of inoculum carried by smaller droplets (Lacey 1996). Our findings that the strongest correlation between high levels of inoculum is found within 5 m from a source are in full agreement with a splash dispersion model (McCartney 1994). This understanding should further assist future studies modeling the dispersal of this pathogen.

The literature on atmospheric dispersal of particles is extensive (reviewed in Van Leuken et al. 2016), and there is a general agreement among authors that analyses of such dispersal are extremely complex and likely to generate theoretical results different from what happens in the real world. Field studies are thus necessary to provide validation and context for the understanding of spread of infectious diseases mediated by spores. This is the first study to experimentally analyze how host composition, host density, rainfall, fog in the absence of rainfall, and temperature may affect sporulation levels and spore dispersal by the SOD pathogen *P. ramorum* in both mixed evergreen and redwood–tanoak stands. The data we collected were instrumental in modeling dynamics of infection from the transmissive host bay to the dead-end host coast live oak. Additionally, results were used for a stand manipulation experiment involving the local removal of bays, which successfully reduced the frequency of events in which inoculum level was high enough to cause oak infection.

Acknowledgments

This study was funded by the "Collaborative Research—Interacting disturbances: leaf to landscape dynamics of emerging disease, fire, and drought in California coastal forests"—Federal Award ID: 1115607 (United States National Science Foundation), the Region 5 FS 10-DG-11052021-230 (United States Department of Agriculture—State and Private Forestry), and the "Reducing the Spread of Sudden Oak Death"—Grant #2639 (Gordon and Betty Moore Foundation).

Literature Cited

Agresti, A. 2001. Exact inference for categorical data: recent advances and continuing controversies. Statistics in Medicine 20:2709–2722.

Akaike, H. 1973. Information theory and an extension of the maximum likelihood principle. Pages 267–

281 *in* B. N. Petrov and F. Csaki, editors. Second International Symposium on Information Theory. Akademiai Kiado, Budapest, Hungary.

Alma, A., C. Marzachì, M. d'Aquilio, and D. Bosco. 2000. Cyclamen (*Cyclamen persicum* L.): a dead-end host species for 16Sr-IB and -IC subgroup phytoplasmas. Annals of Applied Biology 136:173–178.

Balcombe, K. 2005. Model selection using information criteria and genetic algorithms. Computational Economics 25:207–228.

Berbegal, M., A. Pérez-Sierra, J. Armengol, and N. J. Grünwald. 2013. Evidence for multiple introductions and clonality in Spanish populations of *Fusarium circinatum*. Phytopathology 103:851–861.

Box, G. E. P., and D. A. Pierce. 1970. Distribution of residual correlations in autoregressive-integrated moving average time series models. Journal of the American Statistical Association 65:1509–1526.

Browning, M., L. Englander, P. W. Tooley, and D. Berner. 2008. Survival of *Phytophthora ramorum* hyphae after exposure to temperature extremes and various humidities. Mycologia 100:236–245.

Cacuci, D. G., M. Ionescu-Bujor, and I. M. Navon. 2005. Sensitivity and uncertainty analysis. Chapman & Hall/CRC Press, Boca Raton, Florida, USA.

Carsey, T. M., and J. H. Harden. 2014. Monte Carlo simulation and resampling methods for social science. SAGE, London, UK.

Cobb, R. C., R. K. Meentemeyer, and D. M. Rizzo. 2010. Apparent competition in canopy trees determined by pathogen transmission rather than susceptibility. Ecology 91:327–333.

Conover, W. J., and R. L. Iman. 1981. Rank transformations as a bridge between parametric and nonparametric statistics. American Statistician 35:124–129.

Crawley, M. J. 2013. The R book. Second edition. John Wiley & Sons, Chichester, UK.

Croucher, P. J., S. Mascheretti, and M. Garbelotto. 2013. Combining field epidemiological information and genetic data to comprehensively reconstruct the invasion history and the microevolution of the sudden oak death agent *Phytophthora ramorum* (Stramenopila: Oomycetes) in California. Biological Invasions 15:2281–2297.

Davidson, J. M., H. A. Patterson, and D. M. Rizzo. 2008. Sources of inoculum for *Phytophthora ramorum* in a redwood forest. Phytopathology 98:–866.

Davidson, J. M., A. C. Wickland, H. A. Patterson, K. R. Falk, and D. M. Rizzo. 2005. Transmission of *Phytophthora ramorum* in mixed-evergreen forest in California. Phytopathology 95:587–596.

Davis, F. W., D. M. Stoms, A. D. Hollander, K. A. Thomas, P. A. Stine, D. Odion, M. I. Borchert, J. H. Thorne, M. V. Gray, and R. E. Walker. 1998. The California GAP analysis project—final report. University of California, Santa Barbara, California, USA.

Dawson, T. E. 1998. Fog in the California redwood forest: ecosystem inputs and use by plants. Oecologia 117:476–485.

Englander, L., M. Browning, and P. W. Tooley. 2006. Growth and sporulation of *Phytophthora ramorum* in vitro in response to temperature and light. Mycologia 98:365–373.

Eyre, C. A., K. J. Hayden, M. Kozanitas, N. J. Grünwald, and M. Garbelotto. 2014. Lineage, temperature and host species have interacting effects on lesion development in *Phytophthora ramorum*. Plant Disease 98:1717–1727.

Eyre, C. A., M. Kozanitas, and M. Garbelotto. 2013. Population dynamics of aerial and terrestrial populations of *Phytophthora ramorum* in a California forest under different climatic conditions. Phytopathology 103:1141–1152.

Funk, S., H. Nishiura, H. Heesterbeek, W. J. Edmunds, and F. Checchi. 2013. Identifying transmission cycles at the human-animal interface: the role of animal reservoirs in maintaining Gambiense human African trypanosomiasis. PLOS Computational Biology 9:e1002855.

Garbelotto, M., J. M. Davidson, K. Ivors, P. E. Maloney, D. Hüberli, S. T. Koike, and D. M. Rizzo. 2003. Non-oak native plants are main hosts for sudden oak death pathogen in California. California Agriculture 57:18–23.

Garbelotto, M., F. Guglielmo, S. Mascheretti, P. J. Croucher, and P. Gonthier. 2013. Population genetic analyses provide insights on the introduction pathway and spread patterns of the North American forest pathogen *Heterobasidion irregulare* in Italy. Molecular Ecology 22:4855–4869.

Garbelotto, M., T. Y. Harnik, and D. J. Schmidt. 2009. Efficacy of phosphonic acid, metalaxyl-M and copper hydroxide against *Phytophthora ramorum* in vitro and *in planta*. Plant Pathology 58:111–119.

Garbelotto, M., and K. J. Hayden. 2012. Sudden Oak Death: interactions of the exotic oomycete *Phytophthora ramorum* with naive North American hosts. Eukaryotic Cell 11:1313–1323.

Garbelotto, M., E. R. Maddison, and D. Schmidt. 2014. SODmap and SODmap Mobile: two tools to monitor the spread of Sudden Oak Death. Forest Phytophthoras 4: https://doi.org/10.5399/osu/fp.4.1.3560.

Gilbert, J. L. 2007. Insect transmission of plant diseases. Daya Publishing House, New Delhi, India.

Gonthier, P., G. Lione, L. Giordano, and M. Garbelotto. 2012. The American forest pathogen *Heterobasidion irregulare* colonizes unexpected habitats after its introduction in Italy. Ecological Applications 22: 2135–2143.

Gonthier, P., et al. 2014. An integrated approach to control the introduced forest pathogen *Heterobasidion irregulare* in Europe. Forestry 87:471–481.

Goralka, R. J., and J. H. Langenheim. 1995. Analysis of foliar monoterpenoid content in the California Bay Tree, *Umbellularia californica*, among populations across the distribution of the species. Biochemical Systematics and Ecology 23:439–448.

Gramaje, D., M. León, M. Santana, P. W. Crous, and J. Armengol. 2014. Multilocus ISSR markers reveal two major genetic groups in Spanish and South African populations of the grapevine fungal pathogen *Cadophora luteo-olivacea*. PLoS ONE 9:e110417.

Granger, C. W. J. 1969. Investigating causal relations by econometric models and cross-spectral methods. Econometrica 37:424–438.

Grenfell, B. T., and A. P. Dobson. 1995. Ecology of infectious diseases in natural populations. Cambridge University Press, Cambridge, UK.

Grünwald, N. J., M. Garbelotto, E. M. Goss, K. Heungens, and S. Prospero. 2012. Emergence of the Sudden Oak Death pathogen *Phytophthora ramorum*. Trends in Microbiology 20:131–138.

Hesse, W., E. Möller, M. Arnold, and B. Schack. 2003. The use of time-variant EEG Granger causality for inspecting directed interdependencies of neural assemblies. Journal of Neuroscience Method 124:27–44.

Holdenrieder, O., M. Pautasso, P. J. Weisberg, and D. Lonsdale. 2004. Tree diseases and landscape processes: the challenge of landscape pathology. Trends in Ecology & Evolution 19:446–452.

Hosmer, D. W., and S. Lemeshow. 1989. Applied logistic regression. Wiley, New York, New York, USA.

Hüberli, D., B. Lutzy, B. Voss, M. Calver, M. Ormsby, and M. Garbelotto. 2008. Susceptibility of New Zealand flora to *Phytophthora ramorum* and pathogen sporulation potential: an approach based on the precautionary principle. Australasian Plant Pathology 37:615–625.

Johnson, C. 1994. Fruiting of hypogeous fungi in dry sclerophyll forest in Tasmania, Australia: seasonal variation and annual production. Mycological Research 98:1173–1182.

Kasuga, T., M. Kozanitas, M. Bui, D. Hüberli, D. M. Rizzo, and M. Garbelotto. 2012. Phenotypic diversification is associated with host-induced transposon depression in the sudden oak death pathogen *Phytophthora ramorum*. PLoS ONE 7:e34728.

Keesing, F., R. D. Holt, and R. S. Ostfeld. 2006. Effects of species diversity on disease risk. Ecology Letters 9:485–498.

Keesing, F., et al. 2010. Impacts of biodiversity on the emergence and transmission of infectious diseases. Nature 468:647–652.

Kelly, M., and R. K. Meentemeyer. 2002. Landscape dynamics of the spread of sudden oak death. Photogrammetric Engineering & Remote Sensing 68: 1001–1010.

Kilpatrick, A. M., and S. E. Randolph. 2012. Drivers, dynamics, and control of emerging vector-borne zoonotic diseases. Lancet 380:1946–1955.

Lacey, J. 1996. Spore dispersal—its role in ecology and disease: the British contribution to fungal aerobiology. Mycological Research 100:641–660.

Lewis, N. 2013. 100 Statistical tests in R. Heather Hills Press, Ridgmont, UK.

Lione, G., L. Giordano, C. Ferracini, A. Alma, and P. Gonthier. 2016. Testing ecological interactions between *Gnomoniopsis castaneae* and *Dryocosmus kuriphilus*. Acta Oecologica 77:10–17.

Lione, G., L. Giordano, F. Sillo, and P. Gonthier. 2015. Testing and modelling the effects of climate on the incidence of the emergent nut rot agent of chestnut *Gnomoniopsis castanea*. Plant Pathology 64:852–863.

Lione, G., and P. Gonthier. 2016. A permutation-randomization approach to test the spatial distribution of plant diseases. Phytopathology 106:19–28.

Liu, D., M. Kelly, P. Gong, and Q. Guo. 2007. Characterizing spatial–temporal tree mortality patterns associated with a new forest disease. Forest Ecology and Management 253:220–231.

Ljung, G. M., and G. E. P. Box. 1978. On a measure of lack of fit in time series models. Biometrika 65:297–303.

Mascheretti, S., P. J. P. Croucher, M. Kozanitas, L. Baker, and M. Garbelotto. 2009. Genetic epidemiology of the Sudden Oak Death pathogen *Phytophthora ramorum* in California. Molecular Ecology 18:4577–4590.

Mascheretti, S., P. J. P. Croucher, A. Vettraino, S. Prospero, and M. Garbelotto. 2008. Reconstruction of the Sudden Oak Death epidemic in California through microsatellite analysis of the pathogen *Phytophthora ramorum*. Molecular Ecology 17:2755–2768.

McCartney, H. A. 1994. Dispersal of spores and pollen from crops. Grana 33:76–80.

McPherson, B. A., S. R. Mori, D. L. Wood, M. Kelly, A. J. Storer, P. Svihra, and R. B. Standiford. 2010. Responses of oaks and tanoaks to the sudden oak death pathogen after 8y of monitoring in two coastal California forests. Forest Ecology and Management 259:2248–2255.

Meentemeyer, R. K., B. L. Anacker, W. Mark, and D. M. Rizzo. 2008. Early detection of emerging forest disease using dispersal estimation and ecological niche modeling. Ecological Application 18:377–390.

Meentemeyer, R. K., N. J. Cunniffe, A. R. Cook, J. A. N. Filipe, R. D. Hunter, D. M. Rizzo, and C. A. Gilligan. 2011. Epidemiological modeling of invasion in

heterogeneous landscapes: spread of sudden oak death in California (1990–2030). Ecosphere 2:1–24.

Meentemeyer, R. K., M. A. Dorning, J. B. Vogler, D. Schmidt, and M. Garbelotto. 2015. Citizen science helps predict risk of emerging infectious disease. Frontiers in Ecology and the Environment 13:189–194.

Meentemeyer, R., D. Rizzo, W. Mark, and E. Lotz. 2004. Mapping the risk of establishment and spread of sudden oak death in California. Forest Ecology and Management 200:195–214.

Morilla, G., D. Janssen, S. García-Andrés, E. Moriones, I. M. Cuadrado, and E. R. Bejarano. 2005. Pepper (*Capsicum annuum*) is a dead-end host for tomato yellow leaf curl virus. Phytopathology 95:1089–1097.

Ndoumbè-Nkeng, M., M. I. B. Efombagn, S. Nyassé, E. Nyemb, I. Sache, and C. Cilas. 2009. Relationships between cocoa *Phytophthora* pod rot disease and climatic variables in Cameroon. Canadian Journal of Plant Pathology 31:309–320.

Nelson, T. A., and B. Boots. 2008. Detecting spatial hot spots in landscape ecology. Ecography 31:556–566.

Oßvald, W., et al. 2014. Strategies of attack and defence in woody plant-*Phytophthora* interactions. Forest Pathology 44:169–190.

Plantegenest, M., C. Le May, and F. Fabre. 2007. Landscape epidemiology of plant diseases. Journal of the Royal Society Interface 4:963–972.

Poisot, T., J. D. Bever, A. Nemri, P. H. Thrall, and M. E. Hochberg. 2011. A conceptual framework for the evolution of ecological specialisation. Ecology Letters 14:841–851.

R Core Team. 2015. R: a language and environment for statistical computing. R Foundation for Statistical Computing, Vienna, Austria.

Reisen, W. K. 2010. Landscape epidemiology of vector-borne diseases. Annual Review of Entomology 55:461–483.

Ristaino, J. B., and M. L. Gumpertz. 2000. New frontiers in the study of dispersal and spatial analysis of epidemics caused by species in the genus *Phytophthora*. Annual Review of Phytopathology 38:541–576.

Rizzo, D. M., M. Garbelotto, J. M. Davidson, G. W. Slaughter, and S. T. Koike. 2002. *Phytophthora ramorum* as the cause of extensive mortality of *Quercus* spp. and *Lithocarpus densiflorus* in California. Plant Disease 86:205–214.

Sillo, F., L. Giordano, E. Zampieri, G. Lione, S. De Cesare, and P. Gonthier. 2017. HRM analysis provides insights on the reproduction mode and the population structure of *Gnomoniopsis castaneae* in Europe. Plant Pathology 66:293–303.

Silverman, B. W. 1986. Density estimation for statistics and data analysis. Chapman and Hall, London, UK.

Stennett, P. J., and P. J. Beggs. 2004. *Alternaria* spores in the atmosphere of Sydney, Australia, and relationships with meteorological factors. International Journal of Biometeorology 49:98–105.

Swiecki, T. J. and E. A. Bernhardt. 2008. Increasing distance from California bay laurel reduces the risk and severity of *Phytophthora ramorum* canker in coast live oak. Pages 181–194 *in* S. J. Frankel, J. T. Kliejunas, and K. M. Palmieri, editors. Proceedings of the Sudden Oak Death Third Science Symposium. Gen. Tech. Rep. PSW-GTR-214. U.S. Department of Agriculture, Forest Service, Pacific Southwest Research Station, Albany, New York, USA.

Tersago, K., R. Verhagen, O. Vapalahti, P. Heyman, G. Ducoffre, and H. Leirs. 2010. Hantavirus outbreak in Western Europe: reservoir host infection dynamics related to human disease patterns. Epidemiology & Infection 139:381–390.

Van Leuken, J. P. G., A. N. Swart, A. H. Havelaar, A. Van Pul, W. Van der Hoek, and D. Heederik. 2016. Atmospheric dispersion modelling of bioaerosols that are pathogenic to humans and livestock —A review to inform risk assessment studies. Microbial Risk Analysis 1:19–39.

Weaver, S. C., and A. D. Barrett. 2004. Transmission cycles, host range, evolution and emergence of arboviral disease. Nature Reviews Microbiology 2:789–801.

Werres, S., R. Marwitz, W. A. Man In't Veld, A. W. A. M. De Cock, P. J. M. Bonants, M. De Weerdt, K. Themann, E. Ilieva, and R. P. Baayen. 2001. *Phytophthora ramorum* sp. nov., a new pathogen on *Rhododendron* and *Viburnum*. Mycological Research 105:1155–1165.

Wolfowitz, J. 1943. On the theory of runs with some applications to quality control. Annals of Mathematical Statistics 14:280–288.

Worton, B. J. 1989. Kernel methods for estimating the utilization distribution in home-range studies. Ecology 70:164–168.

Yan, H., Q. Liu, M. E. Nelson, and G. G. Grove. 2011. The time lagged effects on the relationship between weather variables and airborne spore concentration of *Erysiphe necator*. Phytopathology 101:S197.

Supporting Information

Additional Supporting Information may be found online at: http://onlinelibrary.wiley.com/doi/10.1002/ecs2.1815/full